

Rotational Relaxation in Polar Solvents. Molecular Dynamics Study of Solute–Solvent Interaction

M. G. Kurnikova, N. Balabai, D. H. Waldeck, and R. D. Coalson*

Contribution from the Department of Chemistry, University of Pittsburgh, Pittsburgh, Pennsylvania 15260

Received August 19, 1997. Revised Manuscript Received March 3, 1998

Abstract: Spectroscopic and molecular dynamics (MD) studies of organic dye molecules in polar solvents are performed to investigate the nature of solute–solvent interactions. Experimental and MD data demonstrate that positively charged molecules rotate more slowly than neutral and negatively charged solutes in polar aprotic solvents. MD simulations of the resorufin, resorufamine, and thionine molecules in DMSO solvent are analyzed to reveal differences in the origins of the frictional forces experienced by each solute molecule. It is demonstrated that specific associations (hydrogen bonds) are formed between the DMSO molecules and both the neutral and the cation solute molecules. No specific solute–solvent association is observed for the negative solute molecule. According to a force separation analysis, the calculated friction on the cation is mostly Coulombic in nature, while it is mostly collisional (mechanical) for the anion case.

I. Introduction

Solvent may influence chemical dynamics in a profound manner.^{1–5} Often, however, the role of the solvent in the mechanism and dynamics of chemical reaction processes which occur in solutions is difficult to disentangle from other influences. Hence, it is desirable to study solute–solvent interactions and relaxation processes for nonreactive systems, so that the solvent's dynamics can be better isolated from the solute dynamics. One probe of these solute–solvent interactions is the rotational relaxation of the solute molecule.^{6–11}

Studies of the rotational relaxation of medium sized, similarly shaped organic dyes^{7–16} in DMSO suggest that positively charged species exhibit longer relaxation times than neutral and negatively charged molecules. For example, the rotational relaxation time of the oxazine cation is 2–3 times longer than that of the resorufin anion.¹² Some of the data from the literature are collected in Table 1. In the present work, new data on the rotational relaxation of two organic cations, thionine and cresyl

Table 1. Rotational Relaxation Times of Organic Dyes in Different Solvents^a

	shape type ^b	DMSO	MeOH	water
anions				
resorufin	1	93	70	61
fluorescein	3	220 [49]	115 [49]	90 [49]
rose bengal	3	340 [49]	—	—
neutral				
resorufamine	1	170 [12]	—	—
nile red	2	228 [7]	76 [7]	150 [7]
cations				
thionine	1	302	84	81
oxazine	1	290 [12]	—	75 [50]
cresyl violet	2	321	110	102
rhodamine 6G	3	480 [48]	133 [52]	210 [51]

^a Time is given in picoseconds. ^b The molecules of type 1 are shown in Figure 1. The molecules of type 2 have a benzene ring fused to the three ring system across the C1–C2 bond. The molecules of type 3 have a carbon in place of the N atom in the central ring and have a phenyl moiety attached to this carbon.

violet, in DMSO, water, and methanol solvents are presented. The data show that the rotational relaxation times of the cations in DMSO solvent are systematically longer than those of similarly shaped anions.^{7,17} A comparison of the rotational relaxation times in the protic solvents, methanol and water, demonstrates that the relaxation times are much more similar in these solvents. Waldeck and co-workers rationalized the trend in DMSO in terms of changes in the “dielectric friction” associated with the different solute species. In contrast to the case of DMSO, the rotational relaxation of the negatively charged dyes in alcohols, for example resorufin¹¹ in ethanol, is observed to be slower than that of the positively charged solutes. This behavior has been explained by the H-bond donating character of the alcohol solvents and solvent association with the solute.¹¹ In the present study, the mechanisms which govern frictional coupling for solute relaxation in a polar solvent are investigated to elucidate these empirical observations concerning the solute–solvent friction.

(17) Jena, A. V.; Lessing, H. E. *Chem. Phys.* **1979**, *40*, 245.

- (1) Bennum, M.; Levine, R. D. *Int. Rev. Phys. Chem.* **1995**, *14*, 215–270.
- (2) Waldeck, D. H. *Chem. Rev.* **1991**, *91*, 415.
- (3) Maroncelli, M. *J. Mol. Liq.* **1993**, *57*, 1–37.
- (4) Hynes, J. T. *Theory of Chemical Reactions*; CRC: New York, 1985.
- (5) Bagchi, B.; Chandra, A. *Adv. Chem. Phys.* **1991**, *80*, 1–127.
- (6) Fleming, G. R. *Chemical Applications of Ultrafast Spectroscopy*; Oxford: New York, 1986.
- (7) Williams, A. M.; Jiang, Y.; Ben-Amotz, D. *Chem. Phys.* **1994**, *180*, 119.
- (8) Dote, J.; Kivelson, D.; Schwartz, R. N. *J. Phys. Chem.* **1981**, *85*, 2169.
- (9) Hartman, R.; Alavi, D.; Waldeck, D. *Israel J. Chem.* **1993**, *33*, 157.
- (10) Alavi, D.; Waldeck, D. In *Understanding Chemical Reactivity*; Kluwer: Amsterdam, 1994.
- (11) Spears, S.; Steinmetz, J. *J. Phys. Chem.* **1985**, *89*, 3623.
- (12) Alavi, D. S.; Hartman, R. S.; Waldeck, D. H. *J. Chem. Phys.* **1991**, *95*, 6770.
- (13) Hartman, R. S.; Konitsky, W.; Waldeck, D. H. *J. Am. Chem. Soc.* **1993**, *115*, 9692.
- (14) Balabai, N.; Waldeck, D. H. *J. Phys. Chem.* **1997**, *101*, 2339.
- (15) Templeton, E. F. G.; Kenney-Wallace, G. A. *J. Phys. Chem.* **1986**, *90*, 5441.
- (16) Philips, L. A.; Webb, S. P.; Clark, J. H. *J. Chem. Phys.* **1985**, *83*, 5811.

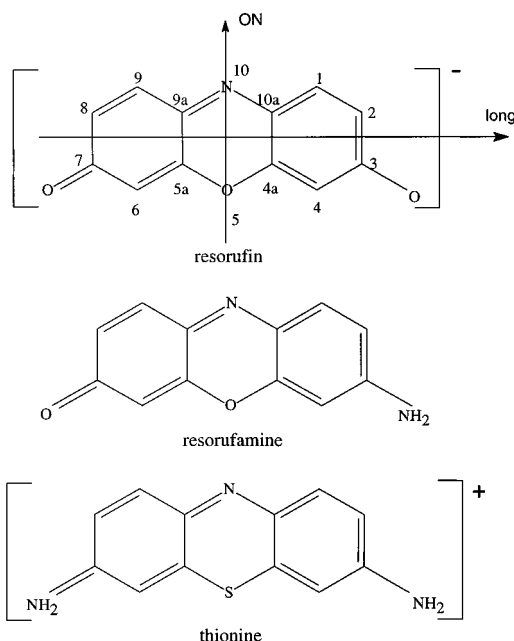


Figure 1. Resorufin (rf), resorufamine (rfm), and thionine (thn) molecules are shown. Two axes of the molecule fixed coordinate system are sketched on the resorufin molecule; the third axis, called norm, is perpendicular to the molecular plane. The indicated numbering scheme for the carbon atoms is used to name the atoms in Figures 4 and 5 and Table 4.

The goal of the present study is to better understand the molecular origins of the difference in frictional coupling between a polar solvent and similarly shaped molecules with different charge distributions. For this purpose, the thionine cation (thn), resorufin anion (rf), and the neutral resorufamine (rfm) molecule (see Figure 1) were examined by means of molecular dynamics (MD) simulations in a model DMSO solvent. The MD method provides a molecular level view of the solute–solvent interactions and the mechanisms which determine the friction experienced by the solute molecules. A recent MD study of resorufamine dynamics in a model dipolar solvent revealed the importance of local solute–solvent interactions for the rotational relaxation mechanism.¹⁸ That study demonstrated the need for a realistic description of the solute–solvent interactions to accurately reproduce the mechanism of the frictional coupling. The present work employs the best available molecular models of the solute and the DMSO solvent.

The MD and experimental results are in qualitative agreement, and it is useful to describe them in the context of a simple hydrodynamic model. In hydrodynamic models for the solute–solvent frictional coupling,^{6–8} the rotational relaxation time τ_{or} may be written as

$$\tau_{or} = (fCV/kT)\eta \quad (1)$$

where η is the shear viscosity, the parameter f accounts for the solute shape, and C is a boundary condition parameter which describes the solute–solvent coupling. In the hydrodynamic model the two extremes for the boundary conditions are referred to as “slip” for weak coupling and “stick” for strong coupling. The room-temperature behavior of the molecules examined here is remarkably dissimilar. Resorufin exhibits a fast, nearly “slip”, rotational relaxation; the resorufamine relaxation is twice as slow, which puts it between the “slip” and “stick” regimes.

(18) Kurnikova, M. G.; Waldeck, D. H.; Coalson, R. D. *J. Chem. Phys.* **1996**, *105*, 628–638.

Thionine relaxes even more slowly than these two and is longer than that predicted by stick; it is in the “superstick” regime. The differences, as demonstrated in this paper, arise mainly from changes in the solute’s ability to associate with DMSO molecules.

The outline of the present manuscript is as follows. Section II describes MD computational details, presents a short discussion of the existing DMSO models and their suitability for the present studies, and introduces the modeled solute molecules. In section III, a brief summary is given of the different approaches to extracting observable quantities such as the rotational reorientation time, the diffusion constant, and the time-dependent friction kernel from the MD trajectory. Section IV reviews the available experimental data and the results of calculating the friction via a continuum model. Section V presents an analysis of the MD simulations performed on resorufin, resorufamine, and thionine molecules in DMSO. Section VI discusses the local solute–solvent interactions and the frictional mechanisms. Concluding remarks comprise section VII.

II. Description of the Models

A. Molecular Dynamics. All MD simulations reported in this paper were produced using the AMBER4.1 program.¹⁹ The Amber force field was modified to include a reaction potential term,²⁰ which accounts for long-range electrostatic interactions. Nonbonded pairwise interactions were calculated explicitly within a 10 Å cutoff radius, and the outside region was treated as a continuum dielectric medium with the dielectric constant $\epsilon_{RF} = 47$. This approach minimizes the size of the box one needs for realistic simulation but treats the long-range forces approximately. Periodic boundary conditions were applied. The following scheme was adopted to perform equilibrium molecular dynamics: (i) short energy minimization of 10 000 steps, (ii) 10-ps constant-pressure MD with a gradual rise of the temperature up to 298 K, (iii) a 40-ps constant-pressure, constant-temperature equilibration MD, and (iv) a constant-volume, constant-temperature ($T = 298$ K) production MD run (1–2 ns). The integration step was 0.5 fs.

The static dielectric permittivity ϵ was determined as²⁰

$$\frac{(\epsilon - 1)(2\epsilon_{RF} + 1)}{(2\epsilon_{RF} + \epsilon)} = \frac{\langle \vec{M}^2 \rangle - \langle \vec{M} \rangle^2}{3\epsilon_0 V k_B T} \quad (2)$$

where \vec{M} is the total dipole moment arising from all DMSO molecules in the simulation cell, $\vec{M} = \sum_i q_i \vec{r}_i$, and the sum runs over all atoms in the box. ϵ_0 is the dielectric permittivity of vacuum. The Debye relaxation time was calculated as²¹

$$\tau_D = \frac{1}{\langle \vec{M}(0)^2 \rangle} \int_0^\infty \langle \vec{M}(t) \cdot \vec{M}(0) \rangle dt \quad (3)$$

B. Model of the Neat DMSO Liquid. A key component of the molecular dynamics method is the availability of a force field which captures the essential physical properties of the system under study. The quality of the solvent model is especially important for the present study since the rotational relaxation of the polar or ionic solute is expected to be very

(19) Pearlman, D. A.; Case, D. A.; Caldwell, J. C.; Seibel, G. L.; Singh, U. C.; Weiner, P.; Kollman, P. A. *AMBER 4.1*, University of California, San Francisco, 1991.

(20) Allen, M. P.; Tildesley, D. J. *Computer Simulation of Liquids*; Clarendon Press: Oxford, U.K., 1987.

(21) McQuarrie, D. A. *Statistical Mechanics*; Harper Collins Publishers: New York, 1976.

Table 2. Properties of DMSO Liquid Calculated by Molecular Dynamics with Different Parameterizations of the Intermolecular Potential

model	τ_D (ps)	τ_{OR} (ps)	D (10^{-4} cm ² s ⁻¹)	ρ (g cm ⁻³)
Rao and Singh ²³	—	1.8	2.8	
Luzar et al. ²⁴	—	3.2	1.7	
Van Gust ²⁵	7.7 ^a	3.9	1.1	1.42 ^a
Fox flex ²²	7.7 ^a	3.3	0.85	1.1 ^a
Fox rigid ²²		6.6	0.5	1.12 ^a
polarizable	5.2 ^a	—	—	1.35 ^a
exptl ²²	19	5.2	0.8	1.099

^a Calculated in the present work (numbers not marked with an *a* are taken from indicated references).

sensitive to both bulk relaxation properties of the solvent and its local relaxation around the solute. The final choice of the “fox flex” DMSO model²² resulted from an investigation of the available DMSO models, as well as an attempt to improve the modeling by introducing a nonadditive polarizable potential field.

Several pairwise additive DMSO potential parameterizations have been reported.^{22–25} The most recent ones^{22,25} can be described as a second generation of DMSO potentials aimed at improving the overall properties associated with the first-generation force fields. All of these models reproduce the heat of vaporization, the density of the liquid, and its structural parameters ($g(r)$) quite well. In general, they underestimate the shear viscosity, diffusion coefficient, and single molecule rotational reorientation time. The last three properties are important in the present study. Table 2 shows the Debye relaxation time (τ_D), rotational reorientation time (τ_{or}), self-diffusion coefficient (D), and the density ρ of the model DMSO solvent as calculated in the present study and reported elsewhere (see the references in Table 2).

The model which exhibits the slowest rotational reorientation time for a solvent molecule is the all atom rigid DMSO model from ref 22. However, the self-diffusion constant obtained from this model is noticeably smaller than the experimental value. In contrast, the flexible all atom model (“fox flex”) gives somewhat poorer agreement with the rotational time but much better agreement with the self-diffusion coefficient. It may be that the improvement in the solvent’s reorientation time for the rigid model, as compared to the flexible model, results from its artificial restriction of the methyl group torsion. This limitation makes the all atom rigid model less appealing than the flexible model.

From Table 2, it is clear that even the second-generation additive two-body interaction potentials for DMSO liquid fail to reproduce some important properties such as τ_{or} and τ_D . It seems that qualitative modification of the model is needed. It has been long appreciated that, despite the ability of additive potentials to accurately reproduce some experimental properties,^{26,27} nonadditive interactions such as the molecular polarizability are critically important for describing polar and ionic interactions.^{28,29} It appears that no polarizable potentials for

Table 3. Nonbonded Parameters Used for the Polarizable DMSO Modeling

atom type	ϵ (kcal/mol)	σ (Å)	Liu et al.	polarizable model	
			Q (e)	Q (e)	α (Å ³)
S	0.310	1.780	0.139	0.111	0.500
O	0.410	1.315	-0.459	-0.367	0.465
CH ₃	0.225	1.830	0.16	0.128	0.878

the DMSO molecule have been reported. At the same time MD simulations performed on other organic liquids indicate that the inclusion of an atomic polarizability term into the force field can effect the relaxation time for different liquids.³⁰ For this reason, an MD simulation of pure DMSO with a polarizable potential was performed. The potential was constructed in the standard manner. The molecule–molecule polarization effect is taken into account by introducing polarizable dipoles at each atomic center. This additional nonadditive term in the force field adds flexibility to the model, which should enable reproduction of various experimental properties in a more natural way. The Liu et al.²⁵ united atom parameters for the DMSO, which exhibits nearly the same properties (especially the same τ_{or}) as those of the “fox flex” model were used as a starting point. The parameters for the polarizable DMSO were prescribed according to AMBER methodology.^{19,30} The use of the united atom model here was essential to make the modeling computationally feasible. The parameters of the Liu et al. model were modified by lowering the atomic partial charges by 20%, and the polarizabilities α were prescribed for each atom in the recommended manner.³⁰ The parameters used are listed in Table 3. The solvent density and rotational relaxation time which this model exhibits are reported in Table 2. As can be seen from the table the effect of including polarizabilities in the model did not lead to improvement in key physical properties.

In view of the above discussion, the all atom flexible DMSO model²² was chosen for the simulation of the rotational relaxation of solute molecules embedded in DMSO solvent. Presently, it appears to be the most suitable DMSO parametrization for investigating the detailed solute–solvent interactions involved in rotational relaxation processes.

The pure DMSO simulation included 342 DMSO molecules. For this model solvent, $\epsilon = 37$ (from eq 2)), which is somewhat smaller than the experimental value of $\epsilon = 47$. τ_D was calculated to be about 7 ps, whereas it is 5.2 ps for the polarizable model (see Figure 2). This number is about two and one-half times smaller than the experimental value.

C. Solute Molecules. The three rigid organic dye molecules resorufin, resorufamine, and thionine have similar shape (see Figure 1) but different electrostatic properties. Resorufin is a negative ion, resorufamine is a neutral polar molecule, and thionine is a monocation. The partial charges and dipole moments on the solute molecules were calculated using the Gaussian94 program.³¹ First a geometry optimization was performed in a vacuum at the Hartree–Fock level with a 3-21G

(22) Fox, T.; Kollman, P. *J. Phys. Chem.* **1997**, submitted for publication.

(23) Rao, B. G.; Singh, U. C. *J. Am. Chem. Soc.* **1990**, *112*, 3803.

(24) Luzar, A.; Soper, A. K.; Chandler, D. *J. Chem. Phys.* **1993**, *99*, 6836.

(25) Liu, H.; Mller-Plathe, F.; van Gunsteren, W. F. *J. Am. Chem. Soc.* **1995**, *117*, 4363–4366.

(26) Jorgensen, W. L.; Tirado-Rives, J. *J. Am. Chem. Soc.* **1988**, *110*, 1657.

(27) Burkert, U.; Allinger, N. L. *Molecular Mechanics*; American Chemical Society: Washington, DC, 1982.

(28) Kistenmacher, H.; Popkie, H.; Clementi, E. J. *J. Chem. Phys.* **1973**, *59*, 5842.

(29) Caldwell, J.; Dang, L. X.; Kollman, P. A. *J. Am. Chem. Soc.* **1990**, *112*, 9144.

(30) Caldwell, J. W.; Kollman, P. A. *J. Phys. Chem.* **1995**, *99*, 6208.

(31) Frisch, M. J.; Trucks, G. W.; Schlegel, H. B.; Gill, P. M. W.; Johnson, B. G.; Robb, M. A.; Cheeseman, J. R.; Keith, T.; Petersson, G. A.; Montgomery, J. A.; Raghavachari, K.; Al-Laham, M. A.; Zakrzewski, V. G.; Ortiz, J. V.; Foresman, J. B.; Cioslowski, J.; Stefanov, B. B.; Nanayakkara, A.; Challacombe, M.; Peng, C. Y.; Ayala, P. Y.; Chen, W.; Wong, M. W.; Andres, J. L.; Replogle, E. S.; Gomperts, R.; Martin, R. L.; Fox, D. J.; Binkley, J. S.; Defrees, D. J.; Baker, J.; Stewart, J. P.; Head-Gordon, M.; Gonzalez, C.; Pople, J. A. *Gaussian 94, Revision C.2*; Gaussian, Inc.: Pittsburgh, PA, 1995.

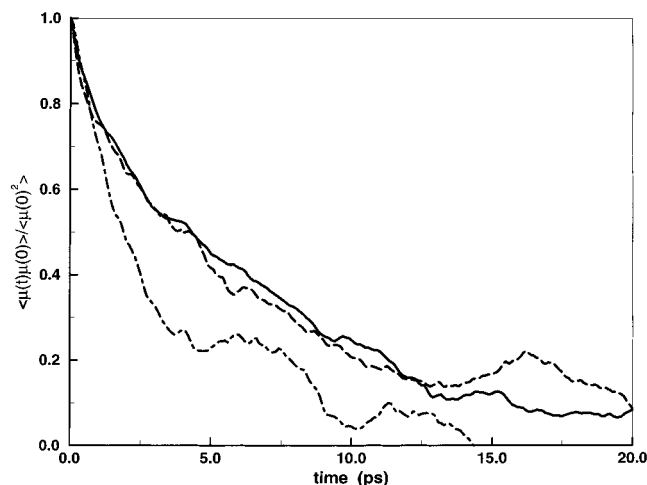


Figure 2. Normalized dipole moment autocorrelation function calculated from the MD trajectories of different DMSO models. The result of the “fox flex”²² parametrization is shown with the solid line. Dashed line is for the united atom model²⁵ and dot-dashed line is for the polarizable DMSO model.

Table 4. Partial Charges on Solute Molecules

resorufin		resorufamine		thionine	
atom name	Q (e)	atom name	Q (e)	atom name	Q (e)
C1	-0.105	C1	-0.071	C1	-0.219
1H	0.198	1H	0.194	1H	0.206
C2	-0.655	C2	-0.680	C2	-0.380
2H	0.244	2H	0.255	2H	0.230
C3	1.060	C3	1.264	C3	0.616
3O	-0.949	3O	-0.900	3N	-0.840
				3NH1	0.425
				3NH2	0.414
C4	-0.915	C4	-0.964	C4	-0.494
4H	0.280	4H	0.288	4H	0.294
C4a	0.550	C4a	0.576	C4a	0.079
O5	-0.420	O5	-0.421	S5	-0.057
C5a	0.550	C5a	0.449	C5a	0.085
C6	-0.920	C6	-0.667	C6	-0.491
6H	0.280	6H	0.276	6H	0.290
C7	1.060	C7	0.662	C7	0.611
7O	-0.950	7N	-0.014	7N	-0.888
		7NH1	0.449	7NH1	0.420
		7NH2	0.428	7NH2	0.422
C8	-0.655	C8	-0.441	C8	-0.374
8H	0.244	8H	0.243	8H	0.227
C9	-0.105	C9	-0.185	C9	-0.194
9H	0.198	9H	0.217	9H	0.201
C9a	0.343	C9a	0.369	C9a	0.582
N10	-0.681	N10	-0.621	N10	-0.739
C10a	0.343	C10	0.292	C10	0.622

basis set. Then the Tomasi³² method was used to incorporate effects of solvation in a dielectric continuum with $\epsilon = 47$ (corresponding to the DMSO dielectric constant). The Merz–Singh–Kollman procedure^{33,34} was employed to fit partial charges to atoms, preserving the calculated value of the dipole moment of the molecules. The partial charges for the solute atoms are listed in Table 4. The transition dipole moments were calculated in a vacuum from the results of configuration interaction singles (CIS) with a 3-21G basis set.

The dye molecules were kept rigid in the course of the simulation by imposing strong torsional constants for the three ring system. Lennard-Jones atom parameters were chosen

(32) Miertus, S.; Tomasi, J. *Chem. Phys.* **1982**, 65, 239.

(33) Besler, B. H.; Merz, K. M.; Kollman, P. A. *J. Comput. Chem.* **1990**, 11, 431.

(34) Singh, U. C.; Kollman, P. A. *J. Comput. Chem.* **1984**, 5, 129.

from the AMBER database. A molecular dynamics run was performed for each dye molecule in DMSO solution according to the scheme described in section A. No counterion was present for the thionine and resorufin. Neglect of the counterion is consistent with the experimental data, in which such small concentrations (10^{-4} M) of the solute are used that ion pairing is not important for studies in pure DMSO.

To estimate a value for the electrostatic contribution to the friction, the MD trajectory of each molecule with the partial charges set to zero (such a noncharged molecule experiences only “mechanical” friction^{10,18,35}) was also evaluated.

III. Theoretical Notes

The anisotropy relaxation experiment measures the molecular orientational correlation function of second-rank $C_2(t) = \langle P_2(\bar{\mu}(t) \cdot \bar{\mu}(0)) \rangle$, where $\bar{\mu}(t)$ is the solute dipole moment vector and $P_2(x)$ denotes the second-rank Legendre function. In general, $C_2(t)$ may have a complicated functional form, but it is usually well fit by a single exponential.^{10,12,15} The $C_2(t)$ correlation function can also be calculated from the MD trajectory. Hence, it is possible to directly compare experiment and theory. The rotational relaxation dynamics of the solute molecule can be described by the generalized Langevin equation³⁶

$$\mathbf{I} \frac{d\bar{\omega}(t)}{dt} = - \int_0^t d\tau \xi(t-\tau) \bar{\omega}(\tau) + \bar{R}(t) \quad (4)$$

where $\bar{\omega}(t)$ is the solute angular velocity, $\bar{R}(t)$ is a random torque, $\xi(t)$ is a memory or friction kernel, and \mathbf{I} matrix is the moment of inertia tensor. For the molecules studied here the diffusion and inertia tensors are nearly diagonal¹⁸ in the molecular coordinate system sketched (see Figure 1). Thus, a component form of the equations will be used with the index i denoting the *long* ($i = 1$), *ON* ($i = 2$), and *norm* ($i = 3$) components of the vector variables and the index ii indicating the diagonal elements of the tensors.

The method used to extract friction coefficients ξ_i from the MD simulation has been described previously.¹⁸ It uses torque-angular velocity cross-correlation functions and angular velocity autocorrelation functions according to the Langevin equation. The time-independent friction coefficient is given by

$$\xi_{ii} = \int_0^\infty \xi_{ii}(t) dt \quad (5)$$

The diffusion coefficient and the friction coefficient are related via the Einstein relation:

$$D_{ii} = kT/\xi_{ii} \quad (6)$$

To connect with experiment, the relaxation time for depolarization of the long axis of an asymmetric ellipsoid was calculated¹⁵ using

$$\tau_{or} = \frac{1}{12} \frac{D_{norm} + D_{ON} + 4D_{long}}{D_{norm}D_{ON} + D_{ON}D_{long} + D_{norm}D_{long}} \quad (7)$$

Within the additive model where only pairwise atom–atom interactions are present, it is legitimate to separate the van der Waals (or mechanical) and electrostatic (or Coulombic) contributions to the total torque, such that

(35) Bruehl, M.; Hynes, J. T. *J. Phys. Chem.* **1992**, 96, 4068.

(36) Mori, H. *Prog. Theor. Phys. (Jpn.)* **1965**, 33, 423.

$$N_i^{\text{vdw}} + N_i^{\text{coul}} = \int_0^t \xi_{ii}^{\text{vdw}}(t - \tau) \omega_i(\tau) d\tau - \int_0^t \xi_{ii}^{\text{coul}}(t - \tau) \omega_i(\tau) d\tau + R_i(t) \quad (8)$$

where N_i^{vdw} is the torque acting on the solute molecule because of the Lennard-Jones solute-solvent interactions and N_i^{coul} is the torque produced by the Coulombic interactions. The “mechanical” (or viscous) contribution to the friction most closely corresponds to $\xi_{ii}^{\text{vdw}}(t)$, which arises from N_i^{vdw} and the dielectric friction is contained in $\xi_{ii}^{\text{coul}}(t)$, which arises from N_i^{coul} . From eq 8, the time-dependent friction produced by the van der Waals and Coulombic forces can be evaluated independently using the procedure described in ref 18. This analysis of the time-dependent friction kernels allows one to separate the total friction experienced by the solute molecule into pieces associated with mechanical and electrostatic forces. This dissection helps to provide a mechanistic understanding of the frictional coupling in polar solvents.

IV. Experimental Section

The time-resolved optical heterodyned polarization spectroscopy technique^{37,38} was used to study the rotational diffusion of the organic solutes. In this technique a linearly polarized pump beam creates an anisotropy in the solution by exciting solute molecules of a particular orientation, and the probe beam detects the relaxation of the anisotropy as a function of time. The experimental setup has been described previously.¹⁴ In this work the rotational relaxation times of thionine and cresyl violet in DMSO, methanol, and water were measured at room temperature. The goal is to create a set of data for solutes with similar shape but different electrostatic properties. Table 1 shows the rotational relaxation times of various solute molecules in three polar solvents. To compare the relaxation rates of similarly shaped species the solute molecules were classified into three different shape types: resorufin-like (Type 1), cresyl violet-like (Type 2), and rhodamine 6G-like (Type 3) molecules (see the explanation in the footnote to Table 1).

Thionine and oxazine, which are positively charged ions, have similar rotation times in all solvents. Resorufin, which is an anion, rotates much faster than the cations in DMSO. However, the relaxation time of resorufin in the protic solvents is much closer to that of cations. In DMSO, the rotational relaxation time of neutral resorufamine lies between the corresponding time for the cations and anions. The same trend in rotational relaxation times is observed for the two other groups. The neutral Nile red rotates faster in DMSO and MeOH than positively charged cresyl violet. Two rhodamine 6G-like dianions fluorescein and rose bengal have shorter relaxation times than the cationic rhodamine 6G in DMSO and water. However, their rotational relaxation times are similar to rhodamine 6G in MeOH. The experimental data suggest that the difference in the rotational dynamics of molecules with similar size and shape is strongly correlated with the electrostatic properties of the solute. The difference in the relaxation times of the anion and the cation is most pronounced in DMSO solvent.

V. Rotational Relaxation Time from MD

Comparison of the results of the thionine, resorufin, and resorufamine MD simulations reveals the following specific

(37) Alavi, D. S.; Hartman, R. S.; Waldeck, D. H. *J. Chem. Phys.* **1991**, *94*, 4509.

(38) Alavi, D. S.; Hartman, R. S.; Waldeck, D. H. *J. Chem. Phys.* **1990**, *92*, 4055.

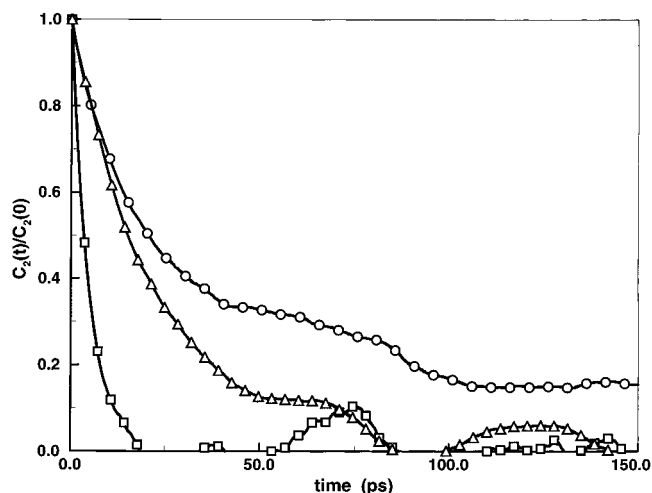


Figure 3. Rotational reorientation correlation functions $C_2(t)$ are shown for thionine (circles), resorufamine (triangles), and resorufin (squares) in the model DMSO solvent.

Table 5. Rotational Relaxation Times from MD

solute molecule	partial charges	τ_{or} (ps)	τ_{orfric} (ps)	τ_{on} (ps)
resorufin	yes	6	10	5
	no	5	6	6
resorufamine	yes	25	31	25
	no	7	6	6
thionine	yes	50	30	27
	no	9	9	8

features of their rotation. The rotational correlation function $C_2(t)$ of the cation (thn) in DMSO decays much more slowly than that associated with the anion (rf). The $C_2(t)$ of the neutral molecule (rfm) has a decay time that lies between the other two (See Figure 3). The observed trend is in agreement with the experimental data (see Table 1).

To compare with the experimental time constants the correlation time τ_{or} was computed as³⁹

$$\tau_{\text{or}} = \int_0^{\infty} C_2(t) dt \quad (9)$$

Table 5 compiles the rotational relaxation times that are calculated from the MD simulations. Comparisons of the τ_{or} time constants in Table 1 and Table 5 show that the MD values are several times smaller than the corresponding experimental values. This discrepancy is partly accounted for by the difference in the dielectric properties of the DMSO model used in MD and those of the real DMSO solvent. On a qualitative level it is clear that the solute rotational relaxation time must be dependent on the solvent relaxation rate. In the context of a continuum model this dependence is captured by the Debye relaxation time and the solvent's dielectric constant. The continuum model¹² yields a factor of 2 decrease in dielectric friction when the values of ϵ and τ_{D} obtained from the MD simulation are used instead of the experimental ones. Other factors that may contribute to the discrepancy between the MD and experimental τ_{or} values are the difference in solvent shear viscosity and limitations in the solute molecule parametrization.

The rotational relaxation obtained from the MD data was also characterized in two other ways. First, the quantity τ_{orfric} , reported in Table 5, was calculated from eqs 6 and 7. Second, the quantity τ_{on} is the decay time, which was calculated as the time constant associated with a single-exponential fit over the

(39) Hansen, J. P.; McDonald, I. R. *Theory of Simple Liquids*; Academic Press: San Diego, CA, 1990.

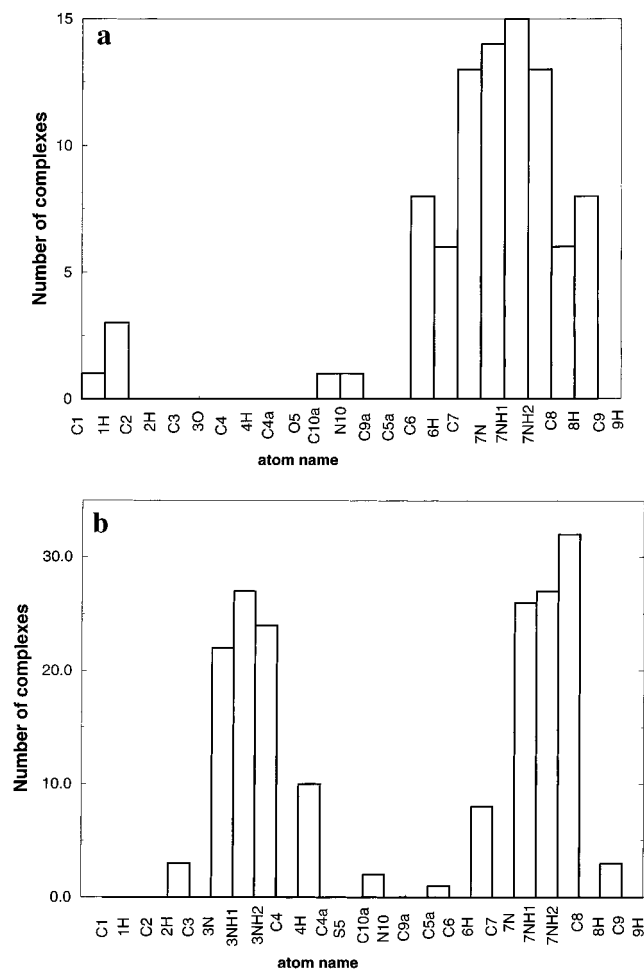


Figure 4. Distributions of the DMSO–solute complexes with different solute atoms (a) for resorufamine and (b) for the thionine.

initial 20-ps span of the $C_2(t)$ correlation function. The three time constants are in good agreement with each other for most cases. An exception is thionine where τ_{or} is larger than τ_{orfric} and τ_{on1} . However, τ_{orfric} and τ_{on1} are close to one another. This discrepancy most probably indicates that the tail of the correlation function was not properly treated because the length of the MD trajectory was insufficient for accurate long-time extraction of $C_2(t)$ for the thionine molecule. The fair agreement among the time constants evaluated using different procedures reflects the fact that all three methods describe the dynamics of the system adequately. In the next section progress is made toward understanding the frictional coupling mechanisms via an examination of the separate roles of electrostatic and collisional friction forces and a structural analysis of the solute–solvent interactions.

VI. Discussion

A. Local Solute–Solvent Interactions. MD trajectories were analyzed to characterize the degree of spatial correlation between the first solvation shell solvent molecules and the solute atomic sites. An elementary event of complex formation between the DMSO and the solute molecule was defined to occur when the O atom of a DMSO molecule remained within 4 Å (i.e., $R_C \leq 4$ Å) of an atom of the solute molecule for a continuous period of time longer than $\tau_c = 20$ ps. This preliminary analysis revealed the existence of long-lived (comparable to the rotation relaxation time) solute–solvent complexes and identified the atomic sites on the solute molecule

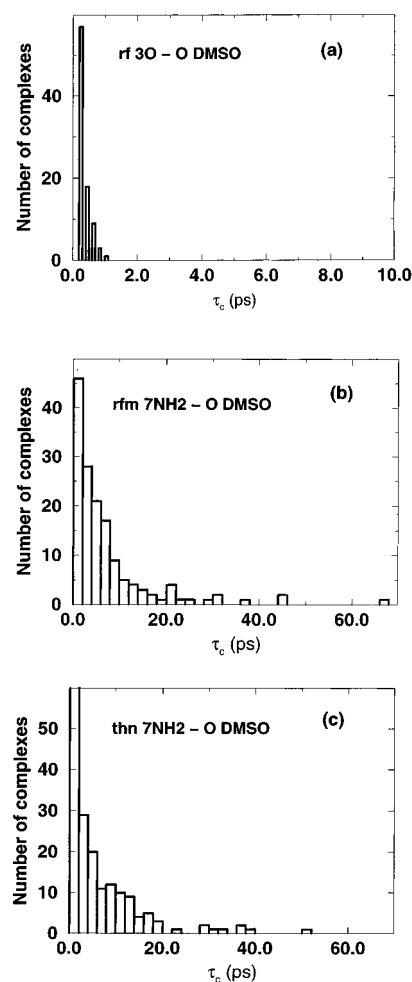


Figure 5. Distribution of lifetimes of the DMSO–solute complexes (a) for resorufin, (b) for resorufamine, and (c) for the thionine.

that attract the DMSO molecules. The distributions of such complexes versus the atom number are shown for resorufamine in Figure 4a and for thionine in Figure 4b. Both histograms display a sharp maximum at the solute atoms which serve as association sites for the DMSO molecules. It is clearly seen from Figures 4 that the resorufamine molecule offers one association site near its NH_2 group, while the thionine molecule supplies two attractive sites for DMSO molecules (both are NH_2 side groups). No complexes were observed for the case of resorufin. By way of contrast, in the reference simulation of the solutes with no charges assigned to atomic sites no complexes were observed.

Having identified the attractive sites of the solute molecule, lifetimes of the solute–solvent associations (hydrogen bonds) were evaluated. This analysis considered all complexes (i.e., $R_C \leq 4$ Å) formed at a particular attractive site (NH_2 moiety) and defined the complexes lifetime τ_c as the amount of time that $R_C \leq 4$ Å. Figure 5 shows histograms of the number of complexes as a function of τ_c . For resorufin this distribution is very sharp (Figure 5a) and is well described by an exponential function with the time constant 0.8 ps. It is clear from this plot that the resorufin does not exhibit a special interaction with DMSO, as reflected in its fast rotational relaxation.

For the NH_2 sites of the resorufamine and thionine molecules the number of complexes observed versus τ_c are plotted in Figure 5, parts b and c, respectively. For resorufamine the distribution of the number of complexes is not a single exponential in time. The initial part of the distribution (up to

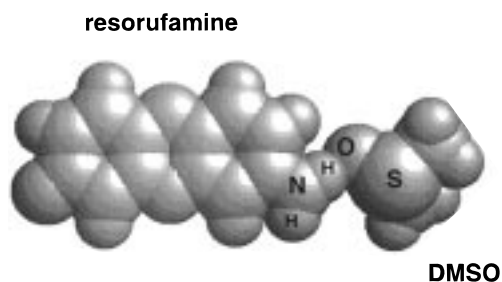


Figure 6. Complex of resorufamine with a DMSO molecule is shown for illustrative purposes.

20 ps) fits well to a single exponential function with a time constant $\tau_c^{\text{short}} = 5$ ps. The time constant of these resorufamine–DMSO complexes is considerably shorter than the rotational relaxation time. The extremely long lived (longer than 20 ps) solute–DMSO associations comprise a second type of complex. The probability that such long lived complexes would occur statistically according to the single-exponential law and Poisson distribution is about one part in 10^6 . An average lifetime of these long-lived complexes was estimated according to

$$\langle \tau_c^{\text{long}} \rangle = \frac{\sum_i N^i \tau_c^i}{\sum_i N^i} \quad (10)$$

where N^i is the number of complexes with the lifetime of τ_c^i . The value of $\langle \tau_c^{\text{long}} \rangle$ is found to be 32 ps, which is similar to the time scale for the rotational relaxation in MD. This analysis indicates that some of the resorufamine complexes can be considered to be stable on the time scale of the rotational reorientation.

Figure 6 shows a representative geometry for a DMSO molecule complexed with the resorufamine molecule. The distance between the O atom of the DMSO molecule and the closest H atom of the resorufamine was 3 Å for the majority of observed complexes. This distance suggests that a weak hydrogen bond^{40–42} is formed between the DMSO and the amino group of the resorufamine. For these stable resorufamine–DMSO complexes, one may consider the complex as a new entity for the rotational relaxation analysis. Such complexes represent a static mechanism for the increase in lifetime from association, a view which is consistent with ideas concerning solvent attachment with a corresponding increase in the solute molecule's hydrodynamic volume.^{11,43} Because of statistical limitations on the MD observations, a more detailed analysis is not justified.

A similar analysis was performed for thionine. Two different configurations of the DMSO molecules around thionine are shown in Figure 7. In this case any number from one to four DMSO molecules was observed to be attached to the two NH_2 groups simultaneously. The analysis of the lifetime distribution, shown in Figure 5c, suggests that for thionine two classes of complex can be identified. The first class has a short lifetime ca. τ_c^{short} , which is obtained from the time constant of an exponential fit to the first 10 ps of the decay. The second class represents longer lived complexes. These complexes were defined starting from 10 ps, which is the time where the histogram in Figure 6c is observed to begin to significantly

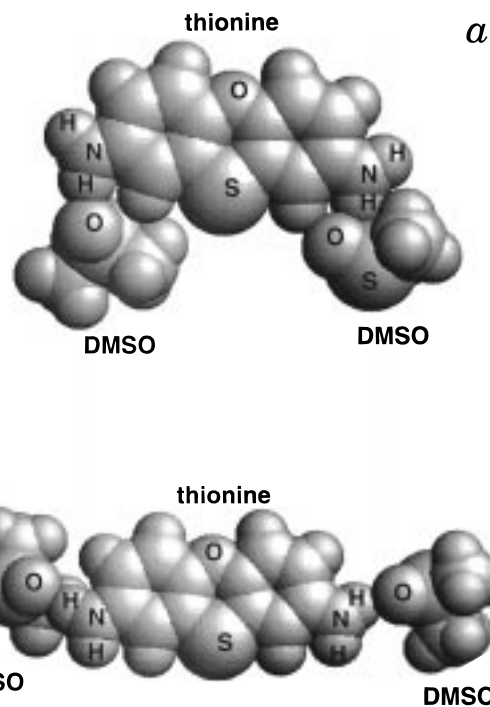


Figure 7. Two configurations of DMSO molecules around thionine are shown.

deviate from a single-exponential decay law. From this analysis, the average lifetime τ_c^{long} of thionine was estimated via eq 10 to be ca. 16 ps. If the average lifetime is computed beginning from 20 ps, as with the resorufamine, the average lifetime τ_c^{long} is 33 ps. The thionine complexes are larger than the resorufamine complexes; however they are more dynamic, i.e. exchange solvent molecules more frequently. Whether the slow rotational relaxation time results from the larger size of the solute caused by solvent association (a static picture) or from an increased drag created by the association and dissociation of solvent molecules as the solute rotates (a dynamic picture) is not clear.

A clear correlation between the ability of the solute to form complexes with the DMSO molecules and the rotational relaxational time of the solute was observed by the above analysis. The slowest molecule, thionine, offered two association sites for the DMSO and was able to attract as many as four DMSO molecules simultaneously, which leads to a large increase in size of the effective complex. By contrast, resorufamine appears to form a stable complex with only one DMSO molecule at a time (as judged by the number of long-lived complexes). The resorufin, which experienced the smallest friction, did not show any signs of complex formation over the course of the simulation.

B. Electrostatic Friction. From the above discussion it is apparent that the ability to associate with DMSO molecules correlates with the trend in the rotational relaxation times for the solutes studied (see Table 5). Figure 8 illustrates this observation. The rotational correlation functions are shown here for each of the model solutes with partial charges (solid line) and without partial charges (open circles) on the atomic sites. The rotational relaxation of all three solutes without partial charges on the atomic sites proceeds on a similar time scale, whereas the relaxation time scales are quite different for these molecules when the partial charges are “turned on”. These data indicate that it is mostly interaction between charges on the solute and solvent molecules which is responsible for association

(40) Jeffrey, G. A. *An Introduction to Hydrogen Bonding*; Oxford University Press: New York, 1996.

(41) Luzar, A.; Chandler, D. *J. Chem. Phys.* **1993**, *98*, 8160.

(42) Benigno, A. J.; Ahmed, E.; Berg, M. *J. Chem. Phys.* **1996**, *104*, 7382.

(43) Zwanzig, R. and Harrison, A. K. *J. Chem. Phys.* **1985**, *83*, 5861.

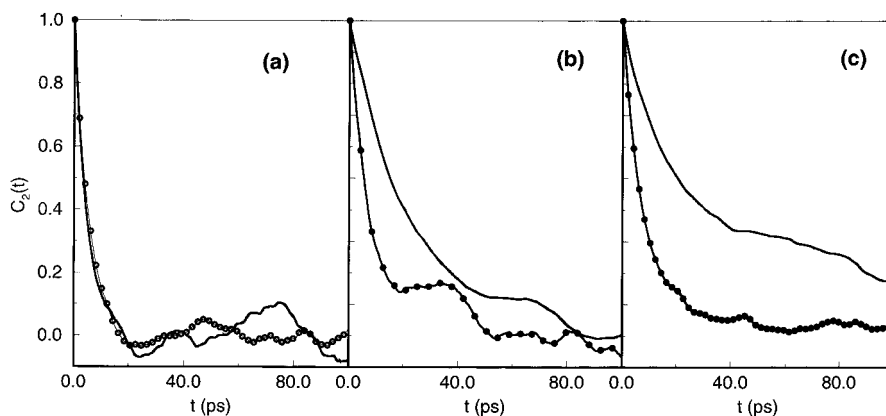


Figure 8. Rotational reorientation correlation functions are shown for the solute molecules with the partial charges on atoms (solid lines) and no partial charges (open circles). Panel a is for resorufin, panel b is for resorufamine, and panel c is for thionine.

with the DMSO and hence the observed difference in the relaxation of the different solutes.

The frictional force which arises because of solute–solvent electrostatic interactions is often associated with the “dielectric friction”. The precise definition of dielectric friction ξ^{df} may vary when discussed by different authors.^{44–47} In MD studies ξ^{df} is sometimes introduced as the difference between the friction on the molecule including partial charges, ξ , and the friction on the same molecule with the charges “turned off”,^{18,35} ξ^0 :

$$\xi^{\text{df}} = \xi - \xi^0 \quad (11)$$

In experimental studies the dielectric friction ξ^{df} is often treated as a term which adds to the viscous friction ξ^{mech} :

$$\xi = \xi^{\text{mech}} + \xi^{\text{df}} \quad (12)$$

Often, ξ^{mech} is calculated according to Stokes Law and ξ^{df} is calculated from an analytical model^{12,44} that is based on a continuum dielectric treatment of the solvent. It is not obvious how to treat the solute solvent frictional coupling when the solute displays complex formation with the solvent. Some authors have proposed defining a hydrodynamic volume for the solute molecule⁴³ which may be larger than the van der Waals volume of the solute molecule. Other workers invoke an additional friction term to account for the “specific” (or local) solute–solvent interactions. In this case, the total friction is written as

$$\xi = \xi^{\text{mech}} + \xi^{\text{specific}} + \xi^{\text{df}} \quad (13)$$

Because the resorufin molecule does not display specific interactions (complex formation) with the solvent in the MD simulation, eq 12 was used to model the friction. The solute molecule was approximated as a smooth asymmetric ellipsoid with axial radii of 6.5:3.5:2 Å.^{14,15} The axial radii were calculated from the bond length and the van der Waals atomic radii. The volume was estimated as the van der Waals volume of the molecule (190 Å³). The mechanical friction on the

Table 6. Contribution from the Mechanical and Dielectric Friction Obtained from Continuum Models and the Experimental Values for Thionine and Resorufin in DMSO

	$\xi^{\text{mech}} (\times 10^{-24} \text{ erg}\cdot\text{s})$			$\xi^{\text{diel}} (\times 10^{-24} \text{ erg}\cdot\text{s})$			τ_{calc} (ps)	τ_{exp} (ps)
	long	ON	norm	long	ON	norm		
resorufin	4.7	24.8	8.6	0.6	7.4	9.2	91	91
resorufamine	4.7	24.8	8.6	1.9	4.4	5.3	74	170
thionine	4.7	24.8	8.6	0.5	14.1	8.4	107	302

molecule was calculated using the Debye–Stokes–Einstein (DSE)²¹ model with a slip boundary condition. Previous work^{6–8} indicates that a slip boundary condition is appropriate for nonpolar solute molecules of this size. The dielectric friction was calculated using the extended charge distribution model⁴⁶ in which the value of the cavity radius was varied until the calculated rotation time for resorufin matched the experimental value. The best fit cavity radius was found to be 6.92 Å (the 10% error bars in the experimental value of τ_{or} results in a range of cavity radii from 6.80 to 7.21 Å).

Because of the geometrical similarity of the thionine and resorufamine with the resorufin molecule, the same parameters (volume and boundary conditions for the viscous friction and cavity radius for the dielectric friction) were used to analyze those data. Using the low and high values for the cavity radius causes a 15% variation in the total rotational relaxation time computed for thionine and resorufamine. The mechanical and dielectric (with a 6.92 Å cavity radius) friction coefficients that are calculated with these parameters are reported in Table 6. In addition the calculated rotational relaxation time is compared to the experimental value for each solute. According to these calculations the dielectric friction is similar for all three molecules. The difference in the observed relaxation time should thus be attributed to the difference in the local solute–solvent interactions, i.e. complex formation.

It is important to realize that the ξ^{df} in eqs 12 and 11 is not necessarily the same because ξ^{mech} is not equal to ξ^0 in a polar solvent. The difference can arise from specific interactions, such as solvent attachment or from changes in the local solvent structure about the solute, that are driven by the solute’s electrostatic field. The change in the mechanical friction of the “charged” molecule versus the “noncharged” molecule, has been discussed previously. The difference between ξ^{mech} and ξ^0 was demonstrated by a previous MD simulation of resorufamine in a model dipolar solvent,¹⁸ where it was shown to arise from structural changes that the solute’s electrostatic potential created for the solvent in the first solvation shell. These effects of the electrostatic field mean that the definition of the dielectric

(44) Nee, T.-W.; Zwanzig, R. *J. Chem. Phys.* **1970**, *52*, 6353.

(45) Hubbard, J.; Onsager, L. *J. Chem. Phys.* **1977**, *67*, 4850.

(46) Alavi, D. S.; Waldeck, D. H. *J. Chem. Phys.* **1991**, *94*, 6196.

(47) Hubbard, J. B. *J. Chem. Phys.* **1978**, *68*, 1649.

(48) Jena, A. V.; Lessing, H. E. *Chem. Phys. Lett.* **1981**, *78*, 187.

(49) Fleming, G. R.; Morris, J. M.; Robinson, G. W. *Chem. Phys.* **1976**, *17*, 91.

(50) Alavi, D.; Waldeck, D. *J. Phys. Chem.* **1991**, *95*, 4848.

(51) Phillion, D. W.; Kuisenga, D. J.; Siegman, A. E. *Appl. Phys. Lett.* **1975**, *27*, 85.

(52) Klein, U. K. A.; Haar, H.-P. *Chem. Phys. Lett.* **1978**, *58*, 531.

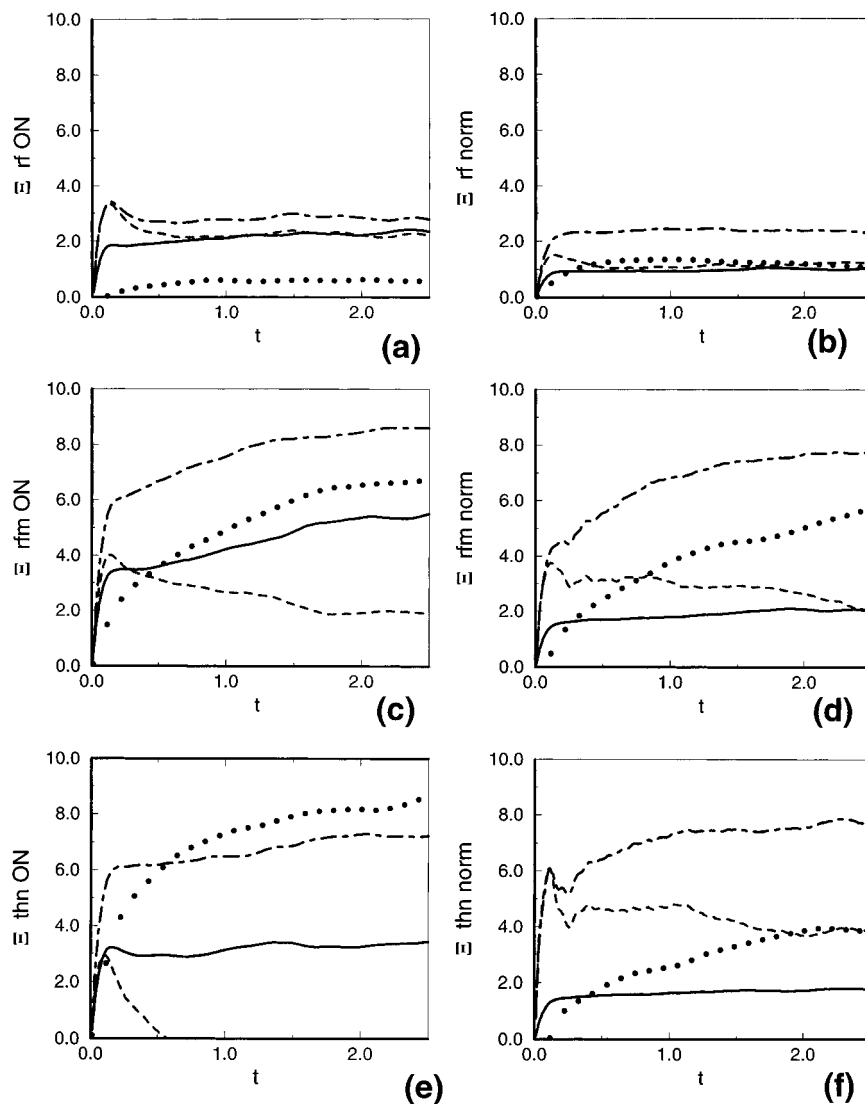


Figure 9. Cumulative integrals of the *ON* (a) and the *norm* (b) components of the friction kernels for the resorufin molecule. The result for total friction is shown with the dot-dashed line, and that for resorufin with no charges is shown with the solid line. The van der Waals component and the Coulombic component of the friction on charged resorufin are shown with the dashed line and the dotted line, respectively. Panels c and d are the same as panels a and b for the resorufamine molecule. Panels e and f are the same as panels a and b for the thionine molecule.

friction given by eq 11 includes local solute–solvent interactions. This definition differs from the conventional definition of the “dielectric friction” as the friction¹⁸ which arises from the phase lag between the solute’s dipole and the dipolar polarization field in the solvent, which is a long range interaction. It is difficult and perhaps not useful to identify the strictly dipolar contributions to the friction because no such solvent exists and the translational modes of the solvent dipoles as well as the specific interactions such as hydrogen bonding will modify the dielectric friction.^{5,45}

C. Force Analysis from MD. What is the nature of the frictional forces responsible for the observed differences in the relaxation rate of the three solute molecules? The ambiguity in the definition of the dielectric friction can be partially removed in the MD analysis if, according to eq 8, one separates the mechanical and electrostatic contributions. To this end the term electrostatic friction is assigned to $\xi_{ii}^{\text{coul}} = \int_0^\infty \xi_{ii}^{\text{coul}}(t) dt$ and the mechanical friction is then associated with the Lennard-Jones forces $\xi_{ii}^{\text{mech}} = \int_0^\infty \xi_{ii}^{\text{vdw}}(t) dt$. With this definition eq 12 becomes exact. In this picture, the difference between ξ_{ii}^{mech} and ξ^0 serves to manifest the coupling between the electrostatic and the mechanical forces in the system. Although this

separation is not conventional, it is useful. In accord with the above definitions the cumulative sums of the van der Waals and Coulombic parts of the friction kernels for rotation of the solute molecules about the *ON* and *norm* axes were constructed as

$$\Xi(t) = \int_0^t \xi(t') dt' \quad (14)$$

The $\Xi(t)$ functions are plotted in Figure 9.

A comparison of the plots in Figure 9 show that the total friction on the resorufin molecule is smaller (about three times) than that for the thionine and resorufamine. In fact, the total friction on the resorufin is comparable to the $\xi_{ii}^{\text{vdw}}(t)$ term for the resorufamine and thionine molecules. The similar rotational relaxation time exhibited by the charged and uncharged resorufin molecules (see Figure 8a) suggests that the resorufin molecule experiences mostly mechanical friction. On the other hand a comparison of the friction kernel integrals in Figure 9a,b indicates that the charged resorufin molecule experiences a somewhat larger friction, especially at the early stages of the relaxation (Figure 9a).

The noticeable difference in the mechanical friction term of the thionine and resorufamine molecules with partial charges, as compared to the friction on the uncharged molecules leads to the conclusion that the charge driven changes in the local solute solvent interactions [as, for example, manifested by the larger mechanical friction in the case of the thionine norm rotation (Figure 9d) and a very large Coulombic friction for the thionine ON rotation (Figure 9c)] are mainly responsible for the larger overall friction experienced by the thionine and resorufamine molecules. This observation is in accord with the analysis of the local solute–solvent association presented in the previous section, since the association was found to be strong for the resorufamine and thionine molecules and absent in the case of the resorufin.

The nontrivial interplay between the Coulombic and the mechanical friction is pronounced for all three molecules. The initial part of the time-dependent cumulative friction rises with time because of the mechanical or short-range forces. This mechanical contribution decreases after about 0.3 ps while the Coulombic part gradually increases. At long time the Coulombic part contributes from one-half to three-quarters of the time-independent friction coefficient for the resorufamine and thionine molecules. The similar behavior of the $\xi_{ii}^{vdw}(t)$ observed for all three solute molecules may result from the structure of the solvent molecule itself. This destructive interaction between the mechanical and Coulomb forces was not observed for the case of resorufamine in a simple diatomic solvent.¹⁸ In that case $\xi_{ii}^{vdw}(t)$ was a monotonically rising function of time until it reached the saturation plateau.

An extreme case of the coupling between the van der Waals and Coulombic friction is observed in Figure 9e for the thionine. After a short time period the mechanical frictional kernel falls down to a negative value, while the Coulombic part grows and dominates the friction after times of 0.5 ps. This extreme case of destructive interference results in a total friction which is smaller than the Coulombic friction.

VII. Concluding Remarks

Spectroscopic and MD studies of organic dye molecules in polar solvents were used to investigate the nature of solute–

solvent interactions. Experimental and MD data demonstrated that positively charged molecules rotate more slowly than neutral and negatively charged solutes in DMSO.

A number of parametrizations of DMSO liquid were explored. None of the available models for the DMSO solvent were able to reproduce τ_D accurately, although the structural properties of the solvent were reproduced well. It seems that the extant pairwise additive models fail to quantitatively account for the intermolecular interactions that are essential for the present study. Polarizable DMSO was also considered but failed to reproduce the experimental value of τ_D . Although the model DMSO was unable to account for the system dynamics on a quantitative level, the qualitative nature of the local intermolecular structure appeared to be correctly described by the model.

The analysis of the MD data on the relaxation of the resorufin, resorufamine, and thionine dyes in DMSO solvent revealed the origin of the differences in the relaxation mechanisms for the three different solute molecules. In particular, the structure and dynamics of solvent–solute hydrogen bonding appear to be important. The slow rotational relaxation of the cation reflects the association of several solvent molecules with the cation. The neutral molecule resorufamine strongly associates with one DMSO molecule and relaxes on a faster time scale than the cation. The association of DMSO about the positively charged and neutral molecule results from the strong solute–solvent electrostatic interaction. In comparison, the rotational relaxation of the anion is relatively fast. In this case, no specific interactions with the DMSO solvent were observed, and therefore, it may be appropriate to describe its rotation in terms of weak coupling continuum models, where the electrostatic interactions are mostly of long range.

Acknowledgment. This work was supported by NSF Grants CHE-9416913 and CHE-9101432. M.G.K. acknowledges the support of a Mellon Predoctoral Fellowship from the University of Pittsburgh. Part of the calculations were carried out on the workstations at the University of Pittsburgh Chemistry Department funded in part by a grant from the National Science Foundation.

JA972926L